Identification of circRNA-miRNA-mRNA Networks to investigate lung adenocarcinoma pathogenesis based on whole-transcriptome analysis

YANG JUAN JUAN (ntdxyjj@ntu.edu.cn)
Affiliated Hospital of Nantong University https://orcid.org/0000-0003-2429-0199

Qian Li
Affiliated Hospital of Nantong University

Yi lu Gu
Affiliated Hospital of Nantong University

Ting ting Bian
Affiliated Hospital of Nantong University

Jiahai Shi
Affiliated Hospital of Nantong University

Yi fei Liu
Affiliated Hospital of Nantong University

Research Article

Keywords: Biomarker, Lung adenocarcinoma, long non-coding RNA, circular RNA, Reference Sequence Database

Posted Date: April 15th, 2022

DOI: https://doi.org/10.21203/rs.3.rs-1559899/v1

Abstract

Background

The progression of lymph node metastasis has been elucidated in lung adenocarcinoma (LUAD), whist which and how transcripts worked in this process remains unclear. We aimed to investigate the markers and potential mechanism of lymph node metastasis in LUAD.

Methods

The whole-transcriptome sequencing was performed on the whole blood from the non-nodal metastasis (LUAD_low), lymph node metastasis (LUAD_high) lung adenocarcinoma patients and healthy people (Control). Subsequently, differential expression analysis among three groups was performed, followed by functional interaction prediction analysis to investigate gene-regulatory circuits in LUAD development. Then, following the rigorous selection, the competing endogenous RNAs (ceRNAs) networks mainly involved in ferroptosis were discovered, and a few of the miRNAs (such as hsa-miR-6509-3p, hsa-miR-6511a-3p, hsa-miR-6803-3p) and their central target gene (*IREB2*) were validated in clinical specimens through qRT-PCR assays.

Results

Our results identified 75 differentially expressed messenger RNAs (dif-mRNAs), 125 differentially expressed microRNAs (dif-miRNAs), and 880 differentially expressed circular RNAs (dif-circRNAs) in non-nodal metastasis LUAD samples compared with Control; similarly, 352 dif-mRNAs, 3 dif-miRNAs, and 270 dif-circRNAs were found in advanced-stage LUAD compared with Control samples. Then the most comprehensive circRNA-associated ceRNA networks were constructed in the pathogenesis and metastasis of LUAD, respectively. Additionally, ferroptosis-associated miRNAs (such as hsa-miR-6509-3p, hsa-miR-6511a-3p, hsa-miR-6803-3p) were both significantly upregulated, whilst their central target gene (*IREB2*) were obviously downregulated in LUAD tissues.

Conclusion

In summary, this study systematically demonstrated circRNA-associated ceRNA profiles in the development of LUAD, which could provide insights that facilitate LUAD diagnosis and therapy in the future.

Introduction

Lung cancer is the most common cause of cancer-related deaths globally, within over 40% of cases being lung adenocarcinoma (LUAD). In recent decades, great progress has been made in improving the

prognosis for non-nodal metastasis LUAD and enhancing the treatment of advanced-stage LUAD [1, 2]; however, the 5-year survival rate of LUAD remains less than 15% [3]. Therefore, increased understanding of its molecular tumor biology and seeking for potential diagnosis marker or therapy target are urgently required.

In recent years, advances in high-throughput next-generation sequencing technologies (NGS) allow us to analyze the progression of cancer based on the characteristics of genome profiles [4, 5]. For example, single-cell transcriptome analysis indicated several exosome markers, such as clusterin and insulin like growth factor binding protein 2 was upregulated in brain metastasis samples compare with primary LUAD samples [6]. ceRNAs represent a novel layer of gene regulation, such as long non-coding RNAs (lncRNAs), small non-coding RNAs (miRNAs), and circular RNAs (circRNAs) usually forms complex ceRNA networks [7–9]. The perturbation of ceRNA crosstalk will disrupt the balance of cellular processes and functions, leading to development of disease including LUAD [9, 10]. Recently, a study reported that LINC00986 acts as a ceRNA to consume miR-21-5p, enhancing the accumulation of SMAD7 and inhibiting cell metastasis [11]; Exosome-derived circRNA_002178 enhanced PD-L1 expression via sponging miR-34, inducing T-cell exhaustion [12]. Additionally, some studies constructed ceRNA regulatory networks in LUAD based on bioinformatics analysis; however, few studies utilized whole-transcriptome sequencing strategies to delineating the transcriptomic landscape of the development of LUAD, including the pathogenesis and metastasis mechanism.

In this study, we performed whole-transcriptome sequencing to analyze the differentially expression of ncRNAs and transcripts among non-nodal metastasis, lymph node metastasis LUAD and healthy cohorts. Subsequently, differential messenger RNA (mRNA), miRNA and circRNA expression analysis was performed, followed by functional interaction prediction analysis. Further, the ceRNA networks mainly involved in ferroptosis was validated in more LUAD samples to confirm the data from NGS.

Methods

Participants and samples

This study was conducted following the criteria of Declaration of Helsinki and approved by the Ethics Committee of Affiliated Hospital of Nantong University. 5 patients with non-nodal metastasis LUAD, 4 with lymph node metastasis and 8 healthy control patients were recruited as the sequencing cohort. In the validation experiments, another 16 LUAD patients and 16 healthy cohorts were recruited.

The diagnosis of lung adenocarcinoma was confirmed following the 2015 World Health Organization (WHO) classification of lung tumors. The healthy controls were recruited from medical examination center of Affiliated Hospital of Nantong University; all the participants were not diagnosed with chronic disease or infection in the last 2 weeks. All patients and healthy controls signed the informed consents, which contained clinical information including age, sex, smoking-history, complications. All the clinical parameters were shown in in Table S1.

Five milliliter whole blood from patients or healthy controls was drawn, and mixed with twenty-five milliliter TRIzol reagent (Invitrogen, Waltham, MA, USA). Then the samples were put into liquid nitrogen for 30 min, and stored at -80℃ until use.

Sequencing process and data analysis

Total RNA from whole blood was exacted according to the protocol of RNAprep Pure Blood Kit (Tiangen Biotech, Beijing, China).The purity and concentration of total RNA were checked by ratio of absorbance at 260 nm and 280 nm; the quality was accessed using Agilent 2100 Bioanalyzer (Agilent Technologies, Santa Clara, CA, USA); finally, the total RNA was verified by electrophoresis on 1% agarose gel.

The preparation of whole transcriptome libraries and deep sequencing were performed by Shanghai Majorbio Corp., Ltd. (Shanghai, China). Whole transcriptome libraries were divided into longRNA-seq and smallRNA-seq libraries, respectively. Sequence reads were aligned to the human genome (GRCh38) (http://asia.ensembl.org/Homo_sapiens/Info/Index) using the Bowiie2 (http://downloads.sourceforge.net/project/bowtie-bio/bowtie2/2.2.9/bowtie2-2.2.9-linux-x86_64.zip), HISAT2 (http://ccb.jhu.edu/software/hisat2/index.shtml), TopHat 2.0 (http://ccb.jhu.edu/software/tophat/index.shtml), and STAR 2.0 (http://code.google.com/p/rna-star/) program. The resulting alignment files were reconstructed with Cufflinks (http://cole-trapnell-lab.github.io/cufflinks/) and StringTieb(http://ccb.jhu.edu/software/stringtie/) program.

The RefSeq and Ensembl transcript databases were chosen as the annotation references for the transcripts annotation. Based on the back splice junction reads, CIRCexplorer [13] was used to predict circRNAs, and the obtained circRNAs was compared with that from circBase and PlantcircBase database. A criterion of data analyses was set as $|\log2FC| \geq 1$ and a p adjust < 0.05 between two groups, so the genes and transcripts accordance to this criteria was identified as differentially expressed genes.

Function annotation and statistical methods

DE genes between non-nodal metastasis and lymph node metastasis LUAD, healthy control were identified via Cuffdiff 2.0. $|\text{fold-change}| \geq 2$, p value < 0.05 and false discovery rate (FDR) ≤ 0.05 was considered statistically significant. NCBI_NR, Swiss-Prot, Pfam, EggNOG, Gene Ontology (GO) and Kyoto Encyclopedia of Genes and Genomes (KEGG) pathway analyses were enriched through the Database for Annotation, Visualization, and Integrated Discovery. Pearson and Spearman algorithm were conducted to assess the correlation between transcripts and to construct the visual networks.

CeRNA network analysis

The expression levels of circRNAs, miRNAs and mRNAs differed significantly separately or both in non-nodal metastasis LUAD, lymph node metastasis LUAD and healthy controls. We used miRanda, TargetScan and RNAhybrid to predict miRNA-binding seed-sequence sites, and an overlap of the same miRNA-binding sites on both circRNAs and mRNAs was indicated as MREs sequence. The whole circRNA-miRNA-mRNA neworks were constructed and visually displayed using Cystoscope software v.3.5.0 (San Diego, CA, USA).

qRT-PCR validation experiments

Whole blood from LUAD patients and healthy controls were exacted using RNAprep Pire Hi-blood Kit (TIAGEN, Beijing, China) according to the manufacture's protocol. After purified, total 2 μg RNAs were reverse-transcribed using EasyScript® One-Step gDNA Removal and cDNA Synthesis SuperMix (TRANS, Beijing, China) and miRNA First Stand cRNA synthesis kit (Sangon Biotech, Shanghai, China), respectively. Then, the levels of transcripts were analyzed by using Hieff® qPCR SYBR Green Master Mix (Low Rox Plus) (Yeasen Biotechnology Co., Ltd, Shanghai, China). GAPDH was used as internal control for mRNA normalization, while U6 was used for miRNA normalization. Relative expression of target genes was calculated using the $2^{-\Delta\Delta CT}$ method.

Statistical Analysis

All the data was described as means ± SD, and analyzed using SPSS version 19.0 software (Chicago, IL, USA). Two-tailed unpaired Student t tests were used to compare the differences between any two groups, and two more distributed groups were compared using ANOVA analysis following Tukey's multiple comparisons test. p value < 0.05 was considered statically significant.

Results

Differential Expression Analysis

We identified 8,031 significantly dysregulated circRNA transcripts between the LUAD_low and Control groups (Fig. 1A; Table S2); of which 3,993 and 4,038 transcripts were upregulated and downregulated in LUAD_low relative to their levels in Control, respectively. Moreover, 7,084 circRNA transcripts were significantly dysregulated in LUAD_high group compared with that in LUAD_low groups, of which 4,228 transcripts were upregulated and 2,856 transcripts were downregulated (Fig. 1B; Table S3). Cluster analysis of the circRNAs expression was conducted, and a heatmap was constructed to visualize the results (Fig. 1C).

Next, based on transcripts per million (TPM) values, 128 significantly dysregulated miRNAs were identified between the LUAD_low and healthy control patients, within 89 upregulated and 39 downregulated miRNAs (Fig. 1D; Table S4). Also 5 miRNAs were significantly dysregulated in LUAD_high patients compared with LUAD_low groups, of which 2 was upregulated and 3 was downregulated (Fig. 1E; Table S5). Cluster analysis of miRNA expression was performed, and a heatmap was generated (Fig. 1F).

In addition, total 111 mRNA transcripts were significantly dysregulated, with 22 and 89 being respectively upregulated and downregulated between LUAD_low and healthy control patients (Fig. 1G; Table S6); 388 mRNAs were significantly dysregulated, with 185 and 203 being upregulated and downregulated in LUAD_high groups (Fig. 1H; Table S7). Once again, cluster analysis was performed on the mRNA expression, and a heatmap was generated (Fig. 1I).

Construction of ceRNA Networks

According to the ceRNA hypothesis, RNA transcripts cross-regulate each other by competing for shared miRNAs. Here, we used our RNA-seq data to construct the ceRNA works in the LUAD development. We divided the differentially expressed transcripts (circRNAs, miRNAs, and mRNAs) into three groups: (1) E yes A no, differential expression in LUAD_low but not in LUAD_high groups. (2) E no A yes, differential expression in LUAD_high patients, but not in LUAD_low groups; and (3) E yes A yes, differential expression both in LUAD_low and LUAD_high groups. The transcripts of the E yes A no, E no A yes, and E yes A yes groups were represent the process for LUAD pathogenesis, LUAD metastasis, and LUAD development, respectively (Figure. 2A).

In the E yes and A no groups, differentially expressed 880 circRNAs and 75 mRNAs shared common MRE binding sites among 125 significantly dysregulated miRNAs (Tables S8). Though a total of 270, 352, and 3 significantly dysregulated circRNAs, mRNAs, and miRNAs were included in the E no A yes group, we found no nodes interactions among these transcripts; finally, 1209 circRNAs, 36 mRNAs, and 2 miRNA were included in the E yes A yes group (Table S9). Figure 2B shows the circRNAs, miRNAs, and mRNAs that were increased, decreased, and increased in E yes A no groups. And Fig. 2C shows the circRNAs, miRNAs, and mRNAs that were decreased, increased, and decreased in E yes A yes groups, these RNA interactions might be critical in LUAD at all stage.

Gene Ontology and Kyoto Encyclopedia of Genes and Genomes Pathway Analysis

To determine the regulation mechanism of ceRNA networks, Gene Ontology (GO) analyses were performed on the circRNA-associated mRNA-encoding genes from above three groups. The top terms in the identified networks from E yes A no group were regulation of cellular process (GO:0050794) and regulation of biological process (GO: 0050789) (Fig. 3A); at the same time, several cell death-associated terms were also observed, such as cell cycle arrest (GO:0071157; GO:0071156; GO:0045787), G0 to G1 transition (GO:0045023), cell division (GO:0051302), and intracellular signal transduction (GO:009996) in E yes A no groups (Table S10).

Additionally, to determine the signaling cascades related to the identified genes, significantly enriched pathways were identified through KEGG pathway analyses. The results showed that the top pathway in the identified network from E yes A no groups were Hippo signaling pathway and microRNAs in cancer (Fig. 3B). In summary, these data suggested that the dysregulation of cell cycle associated genes triggered the formation of LUAD at the early stage. However, since none or an unique ceRNA networks found in the E no A yes and E yes A no groups, respectively, no enriched GO term and KEGG pathway were enriched in this study.

Association study

We selectively analyzed the expression of circRNAs, miRNAs, and their target genes that showed significant differential expression among non-nodal metastasis LUAD and healthy cohorts; moreover, we performed analyses to investigate the most likely relationships between circRNA-associated ceRNA netwok. For example, three identified circRNA (hsa_circ_0123034, hsa_circ_0119549, hsa_circ_0036471) and 19 novel circRNA were found to be a ceRNA of hsa-miR-6511a-3p; hsa_circ_0006374, hsa_circ_0126864, hsa_circ_0036471 were a ceRNA of hsa-miR-6509-3p; hsa_circ_0036471 was a ceRNA of hsa-miR-6803-3p. In addition, the three miRNAs share the same binding sites with iron-responsive element binding protein 2 (*IREB2*), which has been identified as key regulator of iron homeostasis and could cause cellular proliferation in cancer[14] (Fig. 3; Table S10). Therefore, we predict that the identified circRNA-associated ceRNA networks are potentially involved in the pathogenesis of LUAD.

Additionally, we identified another exon-skipping circularization novel circRNA was a ceRNA of hsa-miR-14-3p in the E yes A yes groups; so this data suggested this circRNA-associated ceRNA networks might a key driving factor in the development of LUAD.

Validation of differentially expression mRNAs and miRNAs

To confirm the differentially dysregulated transcripts identified in our RNA-seq data, we selected and analyzed the differentially expression of hsa-miR-6509-3p, hsa-miR-6511a-3p, hsa-miR-6803-3p and their common target *IREB2*. The results indicated that *IREB2* was significantly downregulated in LUAD patients compared with healthy controls; meanwhile, the selected miRNAs levels all increased in LUAD patients. In conclusion, the qPCR results were highly consistent with the RNA-seq data.

Discussion

Although surgical resection and target therapy can improve the prognosis of some LUAD patients, LUAD is still the most mortality disease worldwide. And the small number of useful biomarker makes it challenging to the diagnose and treatment of LUAD at early stage and predict therapeutic effects. Therefore, exploring the novel biomarkers and understanding the mechanism of metastasis of LUADA may provide new tools to treat the disease.

Recently, dysregulated expression of ncRNAs (circRNAs, lncRNAs, miRNAs) was found to be correlated with tumorigenesis and the progression of cancers, whilst the functions of most of these ncRNAs are still a mystery due to the limitation of detection technique and useful databases. Over the traditional sequencing technology, NGS allows us to find novel ncRNAs and to identify tumor driver genes in several types of cancer [15, 16]. In this study, it is the first comprehensive NGS analysis of transcripts profiles including ncRNAs and mRNAS of the development of LUAD, including the non-nodal metastasis LUAD samples, lymph node metastasis LUAD samples, and healthy cohorts. Through comprehensively selected, we found that 75 dif-mRNAs, 880 dif-circRNAs, 125 dif-miRNAs in non-nodal metastasis LUAD samples compared with controls, which supposed to be associated with the pathogenesis of LUAD. Further, the enriched genes in the ceRNA networks that is relevant to the pathological process of LUAD, included regulation of biological process, regulation of cellular process, as well as various pathways,

such as Hippo signaling pathway and microRNAs in cancer. One of these networks involves the gene *IREB2*, a master regulator of iron metabolism that mediates iron uptake, metabolism and storage.

Ferroptosis, a novel form of iron dysregulation induced cell death, is crucial in regulating growth of tumors, such as colorectal cancer, hepatocellular carcinoma, pancreatic cancer, and NSCLC [17–19]. Previous research has suggested that ncRNAs and endogenous ceRNA network mediated ferroptosis drives the lung carcinogenesis. For example, LINC00336 functions as an oncogene to facilitate tumor cell proliferation, inhibit ferroptosis in an ELAVL1-dependent manner in lung cancer [20]; lncRNA P53RRA acts as a potential tumor suppressor by dissociating p53 from a cytosolic Ras GTPase-activating protein-binding protein 1 (G3BP1) complex, inducing cell-cycle arrest and ferroptosis [21]; moreover, lncRNA-MT1DP enhanced the sensitivity NSCLC cells to eartin-induced ferroptosis by regulating the miR-365a-3p/NRF2 signaling pathways[22]. In mammals, iron regulatory proteins (IRPs) post-transcriptionally regulate iron levels by binding to iron responsive elements (IREs). As the iron sensor, *IREB2* directly binds to the RNA stem-loop structures in the 3'-untranslated region (UTR) of mRNA and stabilizes transcripts of iron transporters, such as transferrin receptor protein 1 (TFRC), thereby increasing intracellular iron concentration[23, 24]. *Song et. al* suggested that activation of IREB2-TFRC pathway increases intracellular iron concentration and enhances cell sensitivity to ferroptosis and reinforces host antitumor immunity[25]. In this study, NGS data indicated the expression of *IREB2* was significantly downregulated in non-nodal metastasis LUAD samples compared with controls; similarity, the same lower levels of this gene was validated in 16 more LUAD specimens. Thereby, we hold the hypothesis that the dysregulation of *IREB2*-associated ferroptosis might one of the occurrence factors of LUAD; however, whether it is connected with the metastasis and poor survival needs further study.

Additionally, we found the significant role of upregulated hsa-miR-6509-3p, has-miR-6511a-3p, and has-miR-6803-3p in the mentioned sixteen LUAD samples. Evidence has shown that miR-6509 serves as tumor-suppressive miRNA in cancer. *Fan et al.* reported that lncRNA SNHG6 acted as a ceRNA of miR-6509 for promoting cell proliferation in hepatocellular carcinoma [26]. In this study, miR-6509-3p was found to be in the center of the ceRNA network in the pathogenesis of LUAD and the target miRNA of *IREB2*. Hence, miR-6803-3p and miR-6511a-3p were both upregulated in LUAD and shared the binding sites with *IREB2*, which was consent with the results of miR-6509-3p; however, the role of these two miRNAs was still unclear. Plausibly, miR-6509-3p, miR-6511a-3p, miR-6803-3p may play an important role in the pathogenesis of LUAD. Further mechanistic studies are warranted to determine the miRNA-IREB2 axis in LUAD.

Conclusions

In conclusion, this study explored the molecular mechanism of development of LUAD using whole-transcriptome sequencing and through validation by *in vitro* experiments. The genes, such as *IREB2*, involved in ferroptosis, may play an important role in the pathogenesis of LUAD. Additionally, *IREB2* was the center of ceRNA of three novel miRNAs in LUAD. These findings shed light on the genomic complexity of LUAD and also suggest potential new targets in LUAD characterization. However, this study is limited

by small sample size, so some significantly valuable ceRNA networks were not found between non-nodal metastasis and lymph node metastasis LUAD samples; moreover, the role and the characteristics of dysregulated circRNAs were not validated in the study. Further, *in vivo* validation using an animal model and functional characterization are needed to delineate the exact mechanistic details.

References

1. Doroshow DB, Herbst RS. Treatment of Advanced Non-Small Cell Lung Cancer in 2018. JAMA Oncol. 2018;4(4):569–70.
2. Arbour KC, Riely GJ. Systemic Therapy for Locally Advanced and Metastatic Non-Small Cell Lung Cancer: A Review. JAMA. 2019;322(8):764–74.
3. Bray F, Ferlay J, Soerjomataram I, Siegel RL, Torre LA, Jemal A. Global cancer statistics 2018: GLOBOCAN estimates of incidence and mortality worldwide for 36 cancers in 185 countries. CA Cancer J Clin. 2018;68(6):394–424.
4. Ma YS, Huang T, Zhong XM, Zhang HW, Cong XL, Xu H, Lu GX, Yu F, Xue SB, Lv ZW, et al. Proteogenomic characterization and comprehensive integrative genomic analysis of human colorectal cancer liver metastasis. Mol Cancer. 2018;17(1):139.
5. Javle M, Bekaii-Saab T, Jain A, Wang Y, Kelley RK, Wang K, Kang HC, Catenacci D, Ali S, Krishnan S, et al. Biliary cancer: Utility of next-generation sequencing for clinical management. Cancer. 2016;122(24):3838–47.
6. Liu Y, Ye G, Huang L, Zhang C, Sheng Y, Wu B, Han L, Wu C, Dong B, Qi Y. Single-cell transcriptome analysis demonstrates inter-patient and intra-tumor heterogeneity in primary and metastatic lung adenocarcinoma. Aging. 2020;12(21):21559–81.
7. Ma YS, Yu F, Zhong XM, Lu GX, Cong XL, Xue SB, Xie WT, Hou LK, Pang LJ, Wu W, et al. miR-30 Family Reduction Maintains Self-Renewal and Promotes Tumorigenesis in NSCLC-Initiating Cells by Targeting Oncogene TM4SF1. Mol Ther. 2018;26(12):2751–65.
8. Jiang N, Zou C, Zhu Y, Luo Y, Chen L, Lei Y, Tang K, Sun Y, Zhang W, Li S, et al. HIF-1a-regulated miR-1275 maintains stem cell-like phenotypes and promotes the progression of LUAD by simultaneously activating Wnt/beta-catenin and Notch signaling. Theranostics. 2020;10(6):2553–70.
9. Wu X, Sui Z, Zhang H, Wang Y, Yu Z. Integrated Analysis of lncRNA-Mediated ceRNA Network in Lung Adenocarcinoma. Front Oncol. 2020;10:554759.
10. Tang X, Ren H, Guo M, Qian J, Yang Y, Gu C. Review on circular RNAs and new insights into their roles in cancer. Comput Struct Biotechnol J. 2021;19:910–28.
11. Zhu Y, Bo H, Chen Z, Li J, He D, Xiao M, Xiang L, Jin L, Zhou J, Gong L, et al: **LINC00968 can inhibit the progression of lung adenocarcinoma through the miR-21-5p/SMAD7 signal axis**. *Aging (Albany NY)* 2020, **12**(21):21904–21922.
12. Wang J, Zhao X, Wang Y, Ren F, Sun D, Yan Y, Kong X, Bu J, Liu M, Xu S. circRNA-002178 act as a ceRNA to promote PDL1/PD1 expression in lung adenocarcinoma. Cell Death Dis. 2020;11(1):32.

13. Xiao-Ou Z, Yang H-BW, Zhang X, Lu, Ling-Ling, Chen: **Complementary Sequence-Mediated Exon Circularization**. *Cell* 2014.
14. Boult J, Roberts K, Brookes MJ, Hughes S, Bury JP, Cross SS, Anderson GJ, Spychal R, Iqbal T, Tselepis C. Overexpression of cellular iron import proteins is associated with malignant progression of esophageal adenocarcinoma. Clin Cancer Res. 2008;14(2):379–87.
15. Xu H, Wang C, Song H, Xu Y, Ji G. RNA-Seq profiling of circular RNAs in human colorectal Cancer liver metastasis and the potential biomarkers. Mol Cancer. 2019;18(1):8.
16. Ho DW, Tsui YM, Sze KM, Chan LK, Cheung TT, Lee E, Sham PC, Tsui SK, Lee TK, Ng IO. Single-cell transcriptomics reveals the landscape of intra-tumoral heterogeneity and stemness-related subpopulations in liver cancer. Cancer Lett. 2019;459:176–85.
17. Ye Z, Zhuo Q, Hu Q, Xu X, Mengqi L, Zhang Z, Xu W, Liu W, Fan G, Qin Y, et al. FBW7-NRA41-SCD1 axis synchronously regulates apoptosis and ferroptosis in pancreatic cancer cells. Redox Biol. 2021;38:101807.
18. Chen P, Li X, Zhang R, Liu S, Xiang Y, Zhang M, Chen X, Pan T, Yan L, Feng J, et al. Combinative treatment of beta-elemene and cetuximab is sensitive to KRAS mutant colorectal cancer cells by inducing ferroptosis and inhibiting epithelial-mesenchymal transformation. Theranostics. 2020;10(11):5107–19.
19. Chen P, Wu Q, Feng J, Yan L, Sun Y, Liu S, Xiang Y, Zhang M, Pan T, Chen X, et al. Erianin, a novel dibenzyl compound in Dendrobium extract, inhibits lung cancer cell growth and migration via calcium/calmodulin-dependent ferroptosis. Signal Transduct Target Ther. 2020;5(1):51.
20. Wang M, Mao C, Ouyang L, Liu Y, Lai W, Liu N, Shi Y, Chen L, Xiao D, Yu F, et al. Long noncoding RNA LINC00336 inhibits ferroptosis in lung cancer by functioning as a competing endogenous RNA. Cell Death Differ. 2019;26(11):2329–43.
21. Mao C, Wang X, Liu Y, Wang M, Yan B, Jiang Y, Shi Y, Shen Y, Liu X, Lai W, et al. A G3BP1-Interacting lncRNA Promotes Ferroptosis and Apoptosis in Cancer via Nuclear Sequestration of p53. Cancer Res. 2018;78(13):3484–96.
22. Gai C, Liu C, Wu X, Yu M, Zheng J, Zhang W, Lv S, Li W. MT1DP loaded by folate-modified liposomes sensitizes erastin-induced ferroptosis via regulating miR-365a-3p/NRF2 axis in non-small cell lung cancer cells. Cell Death Dis. 2020;11(9):751.
23. Zumbrennen KB, Wallander ML, Romney SJ, Leibold EA. Cysteine oxidation regulates the RNA-binding activity of iron regulatory protein 2. Mol Cell Biol. 2009;29(8):2219–29.
24. Samaniego F, Chin J, Iwai K, Rouault TA, Klausner RD. Molecular characterization of a second iron-responsive element binding protein, iron regulatory protein 2. Structure, function, and post-translational regulation. J Biol Chem. 1994;269(49):30904–10.
25. Song J, Liu T, Yin Y, Zhao W, Lin Z, Yin Y, Lu D, You F. The deubiquitinase OTUD1 enhances iron transport and potentiates host antitumor immunity. EMBO Rep. 2021;22(2):e51162.
26. Fan X, Zhao Z, Song J, Zhang D, Wu F, Tu J, Xu M, Ji J. LncRNA-SNHG6 promotes the progression of hepatocellular carcinoma by targeting miR-6509-5p and HIF1A. Cancer Cell Int. 2021;21(1):150.

List Of Abbreviations

LUAD, lung adenocarcinoma; NSCLC, non-small cell lung cancer; IRPs□iron regulatory protein; IREs, iron responsive elements; UTRs, untranslated regions; TFRC, transferrin receptor protein 1; IREB2, iron-responsive element binding protein 2; NGS, next-generation sequencing technologies; ceRNAs, competing endogenous RNAs; lncRNAs, long non-coding RNAs; miRNAs, small non-coding RNAs; circRNAs, circular RNAs; mRNAs, messenger RNAs; G3BP1, Ras GTPase-activating protein-binding protein;

Declarations

Ethics approval and consent to participate

This study was approved by the Human Ethics Committee of Affiliated Hospital of Nantong University (access number: 2021-K133). The experimental protocol was established according to the ethical guidelines of the Helsinki Declaration.

Consent for publication

Not applicable.

Competing interests

All authors declare no conflicts of interest.

Availability of data and materials

The datasets used and/or analyzed during the current study are available from the corresponding author on reasonable request.

Funding

This work was supported by the National Natural Scientific Foundation of China (grant. no. 81770266), Nantong Key Laboratory of Translational Medicine of Cardiothoracic Diseases, Jiangsu Post-doctoral Foundation Research Project, China (No. 2019Z142), and Horizontal topic research of Nantong University (No. 21ZH470).

Contributions

Y. F., and J. H., designed the study, supervised the manuscript and provided the finical support. J. J., Y., L, T. T, and Q. L., participated in plasma collection and RNA extraction. J. J., and Y. L., performed the experiments and analyzed the data. J. J., analyzed the results and wrote the manuscript. All authors read and approved the final manuscript.

Conflicts of Interest

The authors declare no competing interests.

Acknowledgements

Not applicable.

Figures

Figure 1

Expression profiles of distinct transcripts

(A-C) Expression profiles of circRNAs. (A and B) In the volcano plots, green, red and gray points represent circRNAs that were downregulated, upregulated, and no significantly different. x axis: log2 ratio of circRNA expression levels. y axis: false discovery rate values (log10 transformed) of circRNAs. (C) Cluster analysis of expression of circRNAs. Red and blue: increased and decreased expression, respectively. (D-F) Expression profiles of miRNAs. (D and E) In the volcano plots, green, red and gray points represent miRNAs that were downregulated, upregulated, and no significantly different. (F) Cluster analysis of expression of miRNAs. Red and blue: increased and decreased expression, respectively. (G-I) Expression profiles of mRNAs. (G and H) In the volcano plots, green, red and gray points represent mRNAs that were downregulated, upregulated, and no significantly different. x axis: log2 ratio of mRNA expression levels. y axis: false discovery rate values (log10 transformed) of mRNAs. (I) Cluster analysis of expression of mRNAs. Red and blue: increased and decreased expression, respectively. C1-C8 represent Control; T10, T9, T7, T5 represent lymph node metastasis LUAD (LUAD_high); T5, T4, T3, T2, T1 represent non-nodal metastasis LUAD (LUAD_low)

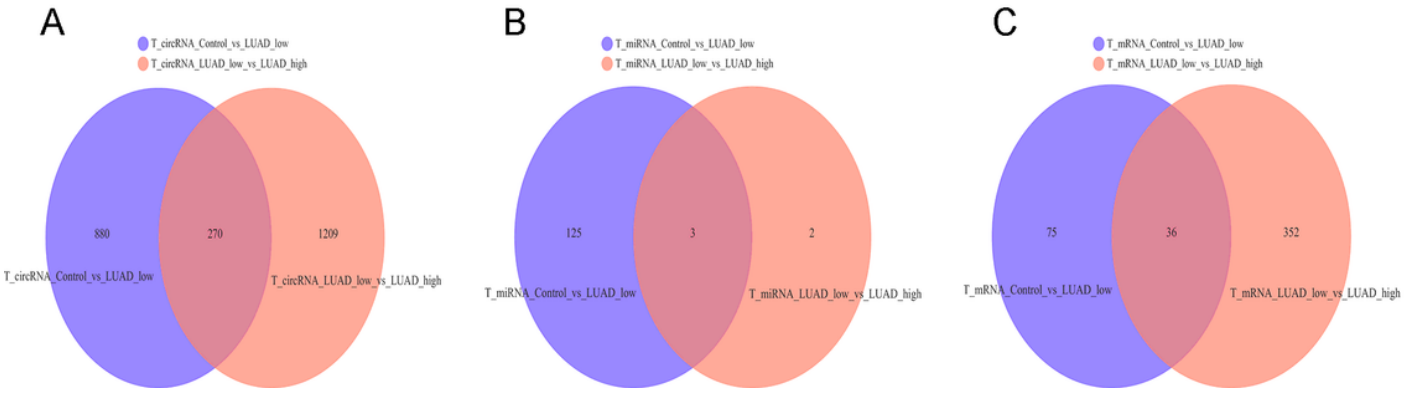

Figure 2

circRNA-associated ceRNA networks in LUAD samples.

The comparative groups were divided into three groups: E yes A no, E no A yes, and E yes A yes groups (A). Further, differentially identified circRNA-miRNA and miRNA-mRNA interactions were used to construct ceRNA networks among E yes A no groups (B) and E yes A yes groups (C).

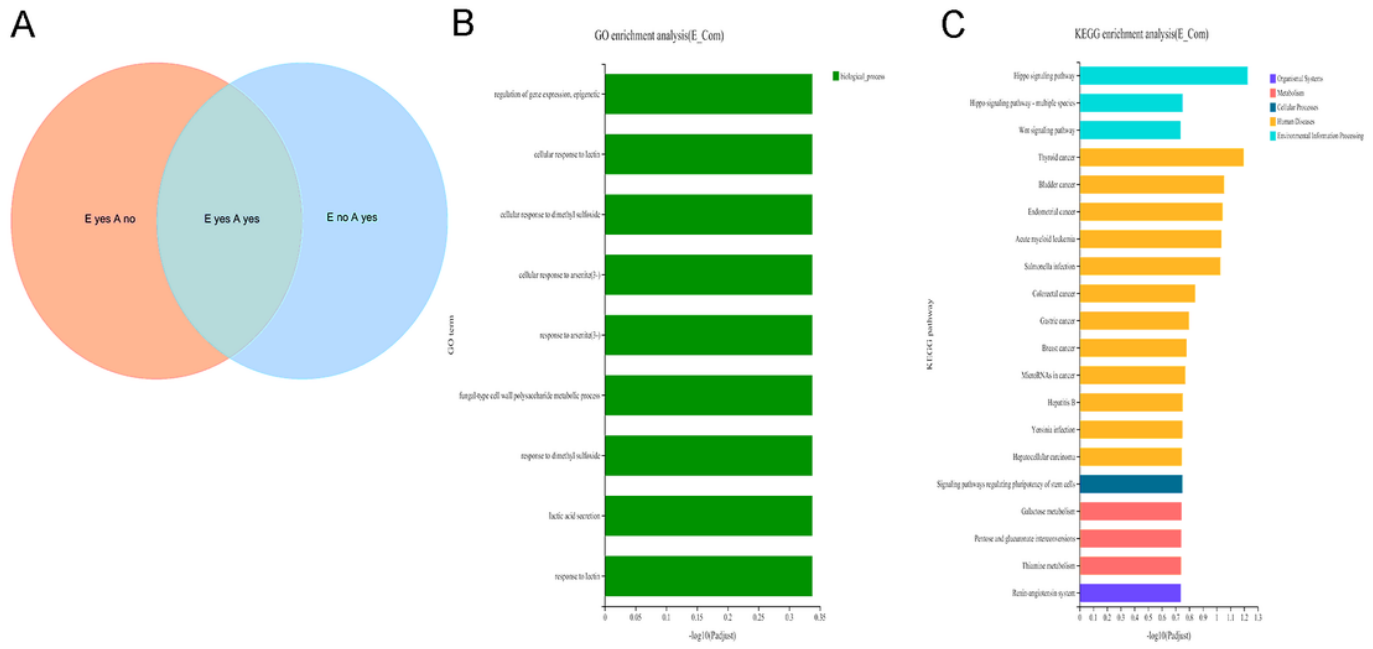

Figure 3

GO enrichment annotation and KEGG pathway analyses.

The top terms of GO enrichment annotation (A) and significantly enriched KEGG pathways (B) of pathological progression of LUAD in E yes A yes groups. All pathways featured p values < 0.05, and the analysis was conducted using the DAVID database.

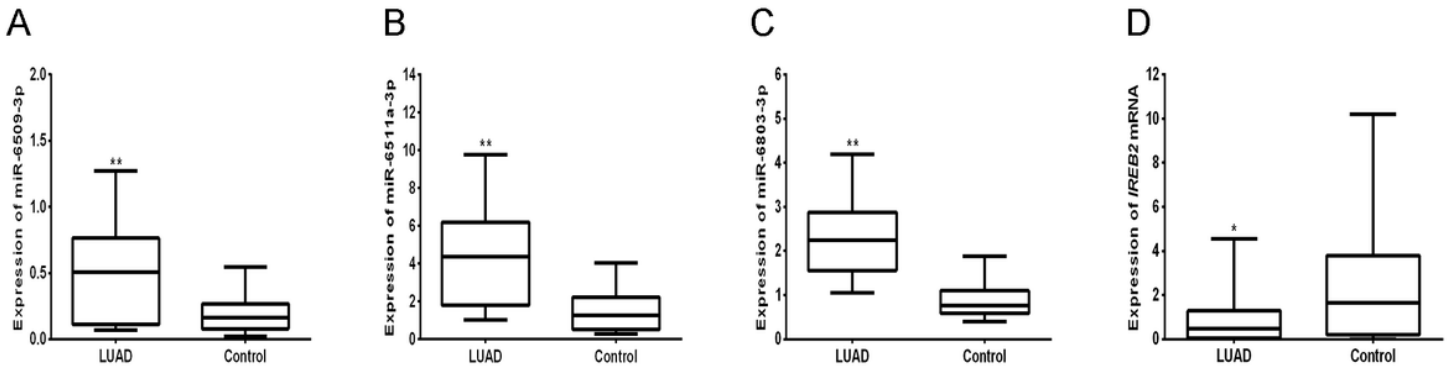

Figure 4

Validation of miRNA and mRNA expression by qPCR.

Levels of miR-6803-3p (A), miR-6511a-3p (B), and miR-6509-3p (C) and *IREB2* (D) LUAD_low and control samples. The miRNAs and mRNA expression were quantified relative to U6 expression level and β-actin,

respectively. Data was shown as means ± SD (n=16; *p<0.05, **p<0.01, compared with Control).

Supplementary Files

This is a list of supplementary files associated with this preprint. Click to download.

- TableS1.xlsx
- TableS2.xls
- TableS3.xls
- TableS4.xls
- TableS5.xls
- TableS6.xls
- TableS7.xls
- TableS8.xls
- TableS9.xls
- TableS10.xls
- Supplementaryinformation.docx